Communications

Automatic Detection of Bioabsorbable Coronary Stents in IVUS Images Using a Cascade of Classifiers

David Rotger, Petia Radeva, and Nico Bruining

***Abstract*—Bioabsorbable drug-eluting coronary stents present a very promising improvement to the common metallic ones solving some of the most important problems of stent implantation: the late restenosis. These stents made of poly-L-lactic acid cause a very subtle acoustic shadow (compared to the metallic ones) making difficult the automatic detection and measurements in images. In this paper, we propose a novel approach based on a cascade of GentleBoost classifiers to detect the stent struts using structural features to code the information of the different subregions of the struts. A stochastic gradient descent method is applied to optimize the overall performance of the detector. Validation results of struts detection are very encouraging with an average *F*-measure of 81%.**

***Index Terms*—Automatic detection, bioabsorbable, cascade, GentleBoost, intravascular ultrasound (IVUS), stent struts.**

I. Introduction

Coronary stents have been widely used in interventional cardiology to scaffold the vessel wall, prevent early elastic recoil and vessel closure, and late constrictive remodeling, as major limitations of balloon angioplasty. However, due to the permanent nature of metallic stents, their presence in a coronary artery poses risks associated with a continuous interaction between the metal and the surrounding tissue resulting in late in-stent neointimal hyperplasia and thrombotic complication [1].

To fulfill the short-term need for vessel scaffolding and avoid potential long-term complications of metallic stents, bioabsorbable polymer stents appear to have the potential of an alternative candidate material. Once they are fully absorbed, only healed vessels are left behind with no residual prosthesis and therefore no potential interactions with the coronary artery. However, bioabsorbable polymer stents have the potential that their radial strength may be lower than that of metallic stents, and thus, more stent recoil might occur after bioabsorbable polymer stent deployment.

The Bioabsorbable Vascular Solutions (BVS) stent is a new type of drug-eluting stent coated with a bioabsorbable polymer containing the antiproliferative drug everolimus, which assesses its safety and feasibility in patients with coronary artery disease (CAD) [2], although there is no information yet regarding long-term recoil property of the BVS after its deployment. We evaluated late recoil of the BVS and assessed its relationship with the stent struts distribution or lesion morphology of stented segments to face the main problems on stent placement that are incomplete stent apposition and in-stent restenosis, showing that the BVS has shrunk in size during the follow-up period. The number of stent struts and lesion morphology of stented segments affected the degree of late stent recoil [3].

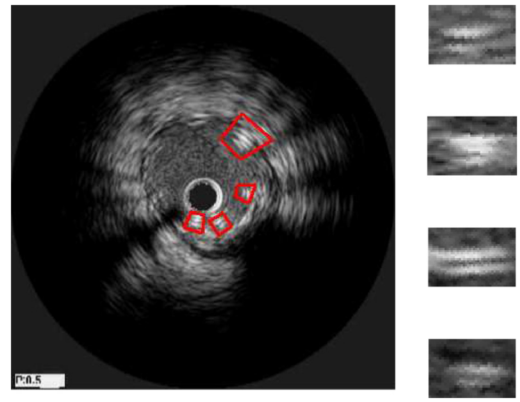

Fig. 1. Vessel with a BVS stent implanted. (Left) IVUS image and stent struts identified (in red). (Right): Polar representation of struts.

Even in the case of high resolution of IVUS images, visual evaluation of stent strut position requires integration of complex information and suffer from substantial variability. There is a strong need for automatic detection and segmentation to provide objective measurements [4], as well as the fusion with other modalities like X-rays [5] and its relationship with vessel dynamics [6]. Texture analysis played a prominent role in computer vision to solve problems of object segmentation and retrieval in numerous applications. Usually, this approach encodes the textural features of images and provides a feature space in which a classification based on such primitives is easier to perform. We propose to employ a cascade of GentleBoost classifiers trained with Haar-like features as an optimal alternative approach for the automatic detection [7] pruning the results using the proximity of the resulting accepted regions to the lumen–intima transition.

In this paper, we present for first time, up to our knowledge, a fully automatic detection scheme for bioabsorbable stent struts in IVUS images used for the evaluation of its late recoil and its relationship with stent struts count and distribution. This scheme consists of struts-like automatic detection using a cascade of GentleBoost classifiers and a prune of the results by automatically detecting the region of maximum likelihood to contain stent struts in IVUS 2-D images. A possible extension to 3-D is under evaluation. A validation scheme is applied measuring the *F*-measure of the detection as well as the interobserver variability based on the Kolmogorov–Smirnov test.

The paper is organized as follows. Section II addresses the methodology for stent struts and maximum likelihood region (MLR) detection, Section III outlines the results and validation, and Section IV presents discussion and conclusions.

II. Methods

A. Stent Struts Detection

Polymer stent struts are represented in IVUS images by two parallel layers of echoes without any acoustic shadowing behind them (see Fig. 1). In order to avoid the deformation of the struts due to their radial localization, we analyze the polar representation of the images.

Manuscript received October 19, 2007; revised November 12, 2008. First published March 16, 2009; current version published March 17, 2010. This work was supported in part by the Project TIN2006-15308-C02 and Project FIS-PI061290 and in part by the Consolider-Ingenio CSD 2007-00018.

D. Rotger is with the Medical Imaging Laboratory (MILab), Computer Vision Center (CVC) and the Computer Science Department, Autonomous University of Barcelona (UAB), 08193 Barcelona, Spain (e-mail: rotger@cvc.uab.cat).

P. Radeva is with MILab, CVC and the Applied Mathematics and Analysis Department, University of Barcelona (UB), 08007 Barcelona, Spain, IEEE member since 1996.

N. Bruining is with the Erasmus Medical Center, Thoraxcenter, 3000 DR Rotterdam, The Netherlands.

Color versions of one or more of the figures in this paper are available online at http://ieeexplore.ieee.org.

Digital Object Identifier 10.1109/TITB.2009.2017528

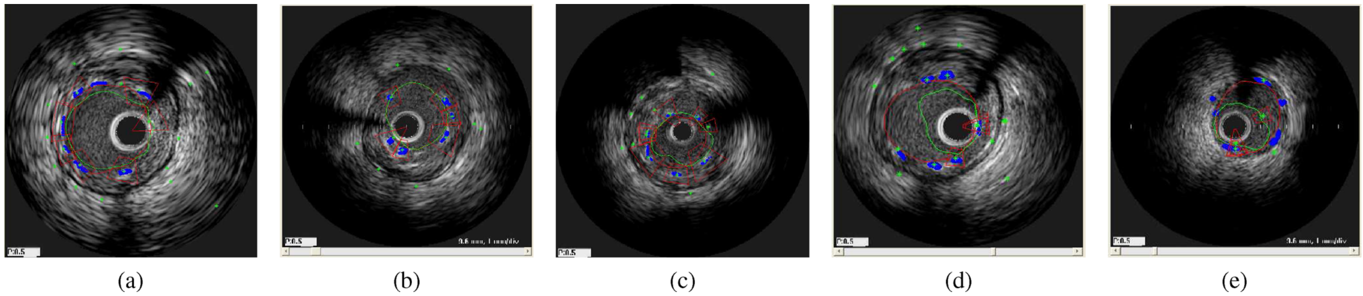

Fig. 2. Struts detection: manual segmentation (red curve), AS of MLR (green curve), central positions of detected stent struts (green stars), struts detected inside the MLR (red boxes), stent struts manually segmented (blue dotted regions).

With these segmented struts and several images of nonstented regions of the vessel as negative samples, we compute a set of Haar-like features and train a cascade of GentleBoost classifiers [7]. The number of stages of the cascade is to be chosen accurately according to the *F*-measure to assure the better performance without loosing sensitivity.

Following the terminology of information retrieval, we employ the precision (P), sensitivity (S), and F-measure (F) defined as

$$P = \frac{\mathrm{TP}}{\mathrm{TP}+\mathrm{FP}} \qquad S = \frac{\mathrm{TP}}{\mathrm{TP}+\mathrm{FN}}$$

where TP is the number of true positives, FP is the number of false positives to be understood as the number of regions that do not intersect any presegmented strut, and FN is the amount of false negatives. In the case of a boosting classifier used as an object detector, several accepted regions can intersect with an object (strut); thus, we need to distinguish between true positive regions (TPRs), which is the number of regions detected that intersects any strut, and true positive detected object (TPO), which is defined as the number of struts that intersects a detected region. Hence, we will use TPR to compute the precision and TPO in the case of sensitivity. By definition of the cascade algorithm, m is defined as the minimum number of neighbor regions detected by the cascade that build up an object (all the groups of a smaller number of rectangles than $m-1$ are rejected, and thus not considered in TPO or TPR).

The *F*-measure can be used as a single measure of the performance of the test as it is defined as the harmonic mean of precision and sensitivity $F = (2\,P\,S)/(P+S)$. In our case, we use a cascade with the *N*-first stages that achieve the highest *F*-measure for all the testings performed on nontraining data.

B. MLR Determination

In order to reduce FP, the previously defined stent struts detection methodology can be refined by adding knowledge based on the probability of a certain region to contain struts. Stent struts are normally located near the region of transition between the lumen (blood) and the tissue (intimal layer). In postimplantation studies, they can be localized inside the lumen area close to its border region, and in the follow-up studies, they can be localized inside the intimal layer and the transition. Thus, we define an MLR as a small region containing the transition lumen–intima.

To automatically segment the lumen border, we train another AdaBoost classifier with several classical textural descriptors and use it as a feature selection method [8] that ensures risk minimization based on minimizing the error on the training set.

We define the MLR as the area contained in the surroundings of the detected lumen border. We refuse all the struts detected with a central position out of the region of maximum likelihood and with an area greater than the maximal strut area of the training set (105 × 70 pixels). Fig. 2 shows examples of the lumen border detected (central line of the MLR) and the strut-like regions detected, accepted, and discarded. Note that the slight discrepancies between the automatic segmentation (AS) and semiautomatic segmentation (SAS) of lumen border do not affect the struts detection.

C. Optimization Based on Stochastic GD

One of the crucial issue of any algorithm is the parameters tuning, in our case, the parameters during the training of the cascade of classifiers. Four of them have been detected as critical for the good performance of the classifier: the false alarm (f) and the hit (h) rates to be used to train each stage of the cascade, the scale factor (s) to scale the search window along the subsequent scans, and the minimum number of neighbor (m) rectangles detected by the cascade to make up an object (all the groups of a smaller number of rectangles than $m-1$ are rejected).

In order to determine the optimal values for these parameters, we apply a stochastic (or online) gradient descent (SGD) [9] based on the minimization of the functional of the *F*-measure, namely $PS(f, h, s, m) = 1 - F$, which defines the performance surface. SGD is a general optimization algorithm, typically used to fit the parameters of a machine-learning model. We follow the "minibatches" form to fit the parameters of the learning and detector algorithms, where the true gradient is approximated by a sum over a small number of training examples. We define a fixed step size for each parameter taking into account the range of plausible values: $f \in [20-50]\%$, $h \in [95-99.5]\%$, $s \in [1.05-1.20]$, and $m \in [1-4]$. Given $m \in N$, the step size is fixed to 25% of the interval size for each parameter.

III. Results

In order to validate our approach, we count with the manual segmentation of two medical experts of the stent struts identified in eight IVUS sequences of 50 images by mean. A total of 1250 struts corresponding to the postimplantation and a follow-up study at six months were performed to five different patients of the Thoraxcenter of the Erasmus Medical Center (Rotterdam, The Netherlands). All the testings are performed following the leave-one-patient-out strategy. The optimal parameters obtained by the SGD for our training set were $f = 0.325, h = 0.995, s = 1.05$, and $m = 1$.

A. Automatic Versus Manual Detection of the MLR

In order to validate the completely automatic stent struts detector, we compare the performance of the algorithms when the MLR is manually delineated versus automatically defined MLR (Section II-B). We analyzed the difference in performance of the previously mentioned

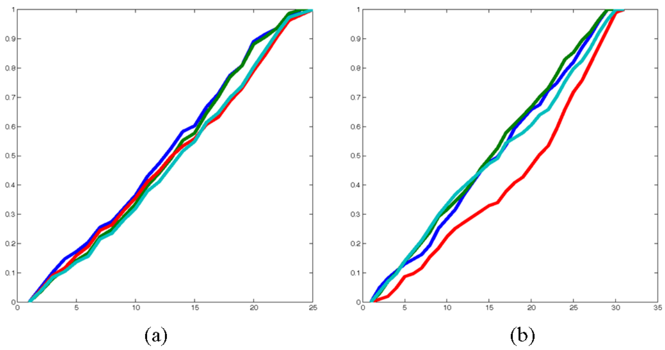

Fig. 3. Normalized cumulative sum of the struts detection with the manual (in green) and the automatic (in blue) MLR detection versus the manual annotation of both experts (in red and cyan) applied to two different patient sequences. (a) Similar shapes denote agreement between observers and the system. (b) Disagreement between experts on that patient case.

classifiers (their F value) between the automatic and the manual detection of the MLR.

Considering all the patient data, we obtain an average $F = 0.79$ using the manual determination of the MLR and $F = 0.71$ using the automatic detection. We noted a decline in performance in the automatic detection results for two patients with respect to the manual ones. While analyzing more carefully these sequences, we noted that the image sequences were modified by the physicians during the acquisition using the IVUS console by zooming and varying the gain of the images. Given that the segmentation algorithm uses texture descriptors, these modifications affect meaningfully the precise detection of the lumen border, and thus the MLR determination. Considering these patients as outliers, we obtained $F = 0.81$ for the manual and $F = 0.75$ for the automatic detection of the MLR. Fig. 2 shows several examples of automatic struts detection following the optimized GentleBoost approach.

B. Assessment of the Struts Detection

In order to assess the ability of our system to describe the concentration and relative position of the stent struts, we must consider: 1) the divergence shown in the segmentation of the same sequence by different specialists (interobserver variability) and 2) comparison to the expert performance (the divergence of the detection of our system in terms of interobserver variability).

In order to perform this analysis, eight sequences were manually segmented by two different specialists independently. A normalized cumulative sum of the number of struts segmented at each image was computed for each sequence. Kolmogorov–Smirnov hypothesis test was performed on these data. The null hypothesis for this test was that normalized cumulative sums of the segmentations provided by the specialists 1 and 2 have the same continuous distribution.

We rejected the null hypothesis if the test was significant at the 95% level. The test resulted negative for all the sequences with a mean p-value of 0.94 ($\pm$0.12). To answer the second question, we performed the same hypothesis tests involving the system output and the segmentations of each specialist. We performed four tests for each sequence corresponding to the system output using AS and SAS of the MLR versus each specialist (see Fig. 3). Low p-values were achieved for the patients considered as outliers in the previous section. The rest of the tests were also rejected, achieving a mean p-value of 0.94 ($\pm$0.13) for the AS tests and 0.95 ($\pm$0.11) in the SAS case.

IV. Discussion and Conclusion

We presented a machine-learning algorithm based on an optimized cascade of multiple classifiers to automatically detect individual stent struts of a very novel bioabsorbable drug-eluting coronary stent in IVUS. The high interobserver variability outlines the difficulty of the fully automatic detection even though the results obtained are within these values of variability.

The determination of the MLR led to be a critical point when changes in illumination and image zoom are performed. Thus, physicians must avoid using it while performing the pullback. Future work will deal with this problem of scaling the image to undo its zoom and tuning the MLR detector with a larger dataset to make it more robust with respect to the variability in gain changes.

References

[1] A. Farb, D. K. Weber, F. D. Kolodgie, A. P. Burke, and R. Virmani, “Morphological predictors of restenosis after coronary stenting in humans,” *Circulation*, vol. 105, no. 25, pp. 2974–2980, 2002.

[2] S. Tanimoto, P. W. Serruys, L. Thuesen, D. Dudek, B. de Bruyne, B. Chevalier, and J. A. Ormiston, “Comparison of in vivo acute stent recoil between the bioabsorbable everolimus-eluting coronary stent and the everolimus-eluting cobalt chromium coronary stent: Insights from the absorb and spirit trials,” *Catheterization Cardiovasc. Interventions*, vol. 70, no. 4, pp. 515–523, 2007.

[3] S. Tanimoto, N. Bruining, R. T. van Domburg, D. Rotger, P. Radeva, J. M. Ligthart, and P. W. Serruys, “Late stent recoil of the bioabsorbable everolimus eluting coronary stent and its relationship with stent struts distribution and plaque morphology,” *J. Amer. Coll. Cardiol.*, vol. 52, no. 20, pp. 1616–1620, 2008.

[4] M. Sonka, X. Zhang, M. Siebes, M. S. Bissing, S. C. Dejong, S. M. Collins, and C. R. McKay, “Segmentation of intravascular ultrasound images: A knowledge based approach,” *IEEE Trans. Med. Imag.*, vol. 14, no. 4, pp. 719–732, Dec. 1995.

[5] A. Wahle, J. J. Lopez, M. E. Olszewski, S. C. Vigmostad, K. B. Chandran, J. D. Rossen, and M. Sonka, “Plaque development, vessel curvature, and wall shear stress in coronary arteries assessed by X-ray angiography and intravascular ultrasound,” *Med. Image Anal.*, vol. 10, no. 4, pp. 615–631, 2006.

[6] S. C. Vigmostad, A. Wahle, M. Olszewski, J. Rossen, M. Sonka, and K. Chandran, “Effects of local geometry on the fluid dynamics of coronary artery segments with implanted stents,” in *Proc. 5th World Congr. Biomech., Munich, J. Biomech. (Suppl.)*, vol. 39, no. 1, p. S401, 2006.

[7] J. Friedman, T. Hastie, and R. Tibshirani, “Additive logistic regression: A statistical view of boosting,” Dept. Stat., Stanford Univ., Stanford, CA, Tech. Rep., 1998.

[8] D. Rotger, P. Radeva, E. Fernández-Nofrerías, and J. Mauri, “Blood detection in IVUS longitudinal cuts using AdaBoost with a novel feature stability criterion,” *Frontiers Artif. Intell. Appl.,* vol. 163, pp. 197–204, 2007.

[9] L. Bottou, “Stochastic learning,” in *Advanced Lectures on Machine Learning* (Lecture Notes in Artificial Intelligence 3176). New York: Springer-Verlag, 2004, pp. 146–168.